Available online at www.sciencedirect.com
ScienceDirect
International Journal of Pharmaceutics 331 (2007) 61–71
INTERNATIONAL JOURNAL OF PHARMACEUTICS
www.elsevier.com/locate/ijpharm

Xanthan–alginate composite gel beads: Molecular interaction and in vitro characterization

Thaned Pongjanyakul [a,*], Satit Puttipipatkhachorn [b]

[a] *Department of Pharmaceutical Technology, Faculty of Pharmaceutical Sciences, Khon Kaen University, Khon Kaen 40002, Thailand*
[b] *Department of Manufacturing Pharmacy, Faculty of Pharmacy, Mahidol University, Bangkok 10400, Thailand*

Received 24 May 2006; received in revised form 24 August 2006; accepted 11 September 2006
Available online 16 September 2006

Abstract

Xanthan gum (XG), a trisaccharide branched polymer, was applied to reinforce calcium alginate beads in this study. Composite beads consisting of XG and sodium alginate (SA) were prepared using ionotropic gelation method. Diclofenac calcium-alginate (DCA) beads incorporated with different amounts of XG were produced as well. Molecular interaction between SA and XG in the composite beads and the XG–DCA beads was investigated using FTIR spectroscopy. Physical properties of the XG–DCA beads such as entrapment efficiency of diclofenac sodium (DS), thermal property, water uptake, swelling and DS release in various media were examined. XG could form intermolecular hydrogen bonding with SA in the composite beads with or without DS. Differential scanning calorimetric study indicated that XG did not affect thermal property of the DCA beads. The DS entrapment efficiency of the DCA beads increased with increasing amount of XG added. The XG–DCA beads showed higher water uptake and swelling in pH 6.8 phosphate buffer and distilled water than the DCA beads. A longer lag time and a higher DS release rate of the XG–DCA beads in pH 6.8 phosphate buffer were found. In contrast, the 0.3%XG–DCA beads could retard the drug release in distilled water because interaction between XG and SA gave higher tortuosity of the bead matrix. However, higher content of XG in the DCA beads increased the release rate of DS. This can be attributed to erosion of small aggregates of XG on the surface of the DCA beads. This finding suggested that XG could modulate physicochemical properties and drug release of the DCA beads, which based on the existence of molecular interaction between XG and SA.

Keywords: Molecular interaction; Calcium alginate bead; Xanthan gum; Diclofenac sodium

1. Introduction

Sodium alginate (SA) is a sodium salt of alginic acid, a naturally occurring non-toxic polysaccharide found in marine brown algae. Alginate has been widely used as food and pharmaceutical additives, such as a tablet disintegrant, a thickening and a suspending agent. It contains two uronic acids, α-L-guluronic and β-D-mannuronic acids, and is composed of homopolymeric blocks and blocks with an alternating sequence (Draget, 2000). Gelation occurs by cross-linking of the uronic acids with divalent cations, such as Ca^{2+}. The primary mechanism of this gelation involves extended chain sequences which adapt a regular two-fold conformation and dimerize with specific chelation of Ca^{2+}, the so-called 'egg-box' structure (Grant et al., 1973). Each Ca^{2+} ion takes part in nine co-ordination link with an oxygen atom, resulting in three-dimensional network of calcium alginate. This phenomenon has been applied for preparing an alginate bead employed as a drug delivery system by dropping the drug-containing SA dispersion into a calcium chloride bath (Østberg et al., 1994; Sugawara et al., 1994). The calcium alginate beads could protect an acid-sensitive drugs from gastric juice, and the drug was consequently released from the beads in the intestine (Hwang et al., 1995; Fernández-Hervás et al., 1998). Thus, drug-loaded alginate beads are suitable for nonsteroidal anti-inflammatory drugs, which caused gastric irritation. Moreover, the alginate beads also exhibited a potential for a pulsatile release system of macromolecular drugs (Kikuchi et al., 1997).

Incorporation of some substances could modify physical properties of calcium-alginate beads. Insoluble substances, such as wax particles (Kim et al., 2005; Pongjanyakul et al., 2006)

* Corresponding author. Tel.: +66 43 362092; fax: +66 43 202379.
E-mail address: thaned@kku.ac.th (T. Pongjanyakul).

0378-5173/$ – see front matter © 2006 Elsevier B.V. All rights reserved.
doi:10.1016/j.ijpharm.2006.09.011

and magnesium aluminum silicate (Puttipipatkhachorn et al., 2005), could improve drug entrapment efficiency and retard drug release from the beads due to an increase in hydrophobic property and an interaction of silanol groups of magnesium aluminum silicate with carboxyl groups of alginate, respectively. Chitin, water-insoluble polymer, was added into the beads so as to retard drug release in pH 6.8 dissolution medium. This was owing to the formation of a complex between the carboxyl groups of alginate and the amino groups of chitin (Murata et al., 2002). Additionally, water-soluble polymers, such as chondroitin sulfate (Murata et al., 1996), konjac glucomannan (Wang and He, 2002), gelatin (Almeida and Almeida, 2004), and sodium starch glycolate (Puttipipatkhachorn et al., 2005), have been also used to reinforce calcium alginate beads because of complex formation of alginate with such water-soluble polymers.

Xanthan gum (XG) is an extracellular polysaccharide secreted by the microorganism *Xanthomonas campestris*. It is complex polysaccharide consisted of a primary chain of β-D-(1,4)-glucose backbone, which has a branching trisaccharide side chain comprised of β-D-(1,2)-mannose, attached to β-D-(1,4)-glucuronic acid, which terminates in a final β-D-mannose (Gruber, 1999). XG has been widely used in oral and topical formulations as a suspending and stabilizing agent (Wade and Weller, 1994), and a release sustaining agent in hydrophilic matrix tablets (Talukdar and Kinget, 1995; Sujja-areevath et al., 1996) and pellets (Santos et al., 2005). Elçin (1995) reported the combination of XG and SA to form spheres for entrapping enzyme in calcium chloride solution. An increase in XG content affected the water uptake of the spheres and this system could still retain the enzyme activity entrapped. However, no data reported about other physicochemical properties of this system. Recently, XG has been also used to combine with SA and zinc acetate in matrix tablets to enhance viscosity of swollen alginate matrix so that zinc ions could interact with alginate to form zinc alginate, resulting in retarding drug release (Zeng, 2004).

In the present study, we intended to prepare composite beads consisting of SA and XG, and diclofenac calcium alginate (DCA) beads reinforced with different amounts of XG by using ionotropic gelation method and using calcium ion as a cross-linking agent. Molecular interaction of XG and SA in the beads was investigated using FTIR spectroscopy. Moreover, physicochemical properties of the XG-DCA beads, such as entrapment efficiency of diclofenac sodium (DS), thermal behavior, water uptake, swelling, and drug release in various dissolution media were investigated as well.

2. Materials and methods

2.1. Materials

Diclofenac sodium (DS) was a gift from Biogena Ltd. (Limassol, Cyprus). Sodium alginate NF17 and xanthan gum were purchased from Srichand United Dispensary Co., Ltd. (Bangkok, Thailand) and Nam Siang Co., Ltd. (Bangkok, Thailand). All other reagents used in this study were of analytical grade and used as received.

2.2. Bead preparation

SA (1.5%, w/v) and XG (0.3, 0.5 and 1.0%, w/v) were dispersed in distilled water. XG–SA dispersion (80 ml) was dropped through a 1.2 mm inner diameter needle, from hypodermic syringe into 0.45 M calcium chloride solution (200 ml). The composite gel beads were cured in this solution for 1 h, then filtered, and rinsed several times with distilled water. The beads were dried at room temperature for 48 h, followed at 45 °C for 12–16 h. To prepare the DCA beads, DS (1%, w/v) was added into the dispersion and completely dissolved with a homogenizer for 5 min before cross-linking process, and then the preparation was proceeded as described above.

2.3. Rheological studies of composite dispersions

Rheological properties and viscosity of SA and XG–SA dispersions at the concentration used in Section 2.2 was studied using small sample adapter of Brookfield Digital Rheometer (Model DV-III, Brookfield Engineering Labs. Inc., Stoughton, MA) at 32 ± 1 °C. A rheogram of the samples was obtained by plotting between shear rate and shear stress from various revolution rates when a spindle (no. 34) was used. To characterize the type of flow of the samples, the following exponential formula was used (Martin, 1993):

$$F^N = \eta G \quad (1)$$

$$\log G = N \log F - \log \eta \quad (2)$$

where F, G, N, and η are shear stress, shear rate, exponential constant and viscosity coefficient, respectively. Rheological properties of 1% (w/v) XG dispersion could not be characterized by using this condition because it had too high viscosity.

2.4. Fourier transformed infrared (FTIR) spectroscopy

FTIR spectra of DS, SA, XG, calcium alginate beads and DCA beads were recorded with a FTIR spectrophotometer (Spectrum One, Perkin Elmer, Norwalk, CT) using KBr disc method. Each sample was gently triturated with KBr powder in a weight ratio of 1:100 and then pressed using a hydrostatic press at a pressure of 10 tons for 5 min. The disc was placed in the sample holder and scanned from 4000 to 450 cm^{-1} at a resolution of 4 cm^{-1}.

2.5. Particle size determination

Particle size of the DCA beads was determined using an optical microscope (Nikon, Japan). Two hundreds fifty beads were randomized and their Feret's diameters were measured and the mean diameters were calculated.

2.6. Drug content determination

Weighed DCA beads were immersed and dispersed in 100 ml of 0.067 M phosphate buffer at pH 6.8 for 12 h. Then, the solution was filtered, and the DS content was assayed by a

UV-spectrophotometer (Shimadzu UV1201, Kyoto, Japan) at wavelength of 260 nm. The ratio of the actual to the theoretical drug contents in the DCA beads was termed as entrapment efficiency (Wang and He, 2002).

2.7. Scanning electron microscopic studies

Surface morphology of the DCA beads was characterized before and after release testing in distilled water. Samples of the dried beads were mounted onto stubs, sputter coated with a gold in a vacuum evaporator, and photographed using a scanning electron microscope (Jeol Model JSM-5800LV, Tokyo, Japan).

2.8. Differential scanning calorimetry (DSC)

DSC thermograms of DS, SA, XG, calcium alginate bead and DCA bead were recorded using a differential scanning calorimeter (DSC822, Mettler Toledo, Switzerland). Each sample (2–2.5 mg) was accurately weighed into a 40-μl aluminum pan without an aluminum cover. The measurement was performed between 30 and 350 °C at a heating rate of 10 °C/min.

2.9. Water uptake determination

Weighed DCA beads were placed in a small basket, soaked in 0.067 M phosphate buffer at pH 6.8 or distilled water and shaken occasionally at room temperature (26 ± 1 °C). After a predetermined time interval, each basket was withdrawn, blotted to remove excess water and immediately weighed on an analytical balance (Remuñán-López and Bodmeier, 1997). The water uptake can be calculated from the following equation:

$$\text{water uptake (\%)} = \left(\frac{W_t - W_0}{W_0}\right) \times 100 \quad (3)$$

where W_t and W_0 are the wet and initial mass of beads, respectively. Water uptake study of DCA beads in pH 6.8 phosphate buffer was performed for 45 min because the swollen beads were broken and could not be blotted to remove an excess water at the longer time.

2.10. Swelling studies

The diameter of DCA beads were measured using a digital caliper (Mitutoyo Model 500-136, Kawasaki, Japan) and then placed in petri disk containing 20 ml of 0.067 M phosphate buffer at pH 6.8 or distilled water at room temperature (26 ± 1 °C). At predefined time intervals, the diameter of each bead was determined at two different positions, and swelling (%) of the beads was calculated according to Eq. (4) (Talukdar and Kinget, 1995).

$$\text{swelling (\%)} = \left(\frac{D_t - D_0}{D_0}\right) \times 100 \quad (4)$$

where D_0 and D_t are the initial diameter of the beads and the diameter of the beads at a given time, respectively.

2.11. In vitro drug release studies

A USP dissolution apparatus I (Hanson Research, Northridge, CA) was used to characterize the release of DS from the DCA beads. The baskets were rotated at 50 rpm at 37.0 ± 0.5 °C. The dissolution media used were 0.067 M phosphate buffer at pH 6.8 or distilled water. The amount of the DCA beads added to 750 ml dissolution medium was equivalent to DS 25 mg. Samples (7 ml) were collected and replaced with a fresh medium at various time intervals. The amount of drug released was analyzed spectrophotometrically at 260 nm (Shimadzu UV1201, Japan). Matrix erosion after release testing in distilled water was also determined using the following equation:

$$\text{matrix erosion (\%)} = \left(\frac{W_0 - W_d - W_r}{W_0}\right) \times 100 \quad (5)$$

where W_0 is the initial mass of the beads, W_d the dry beads mass after release study, and W_r is the total amount of DS released.

The DS release kinetics from the DCA beads in various dissolution media were investigated by fitting the DS release data into zero order and Higuchi's model, which can be expressed using Eq. (5) as followed:

$$Q = kt^n \quad (6)$$

where Q is the percentage of drug released at a given time (t), k the release rate and n is the diffusion exponent. The n value could be defined as 0.5 and 1, which indicated the Higuchi's and zero order equation, respectively (Costa and Lobo, 2001). The release rate was estimated by fitting the experimental drug release data into both models and analyzed by linear regression analysis.

2.12. Statistical analysis

One-way analysis of variance (ANOVA) with the least significant difference (LSD) test for multiple comparisons (SPSS program for MS Windows, release 10.0) was performed to determine the significant effect of DS entrapment efficiency, water uptake, swelling and release parameter of the DCA beads, and viscosity parameters of dispersions. Difference were considered to be significant at a level of $P < 0.05$.

3. Results and discussion

3.1. Effect of XG on rheology and viscosity of SA dispersion

Interaction of SA with XG in dispersion was studied by examining a change in rheology and viscosity of the composite dispersions. Rheograms of SA and XG–SA composite dispersions are shown in Fig. 1. It can be seen that relationship between shear rate and shear stress of SA and XG–SA dispersions showed a straight line, whereas non-linear curve of 0.3% and 0.5%XG dispersions was found. The rheological parameters of all dispersions are listed in Table 1. N values of SA and XG–SA dispersions were in the range of 0.93–1.01, suggesting

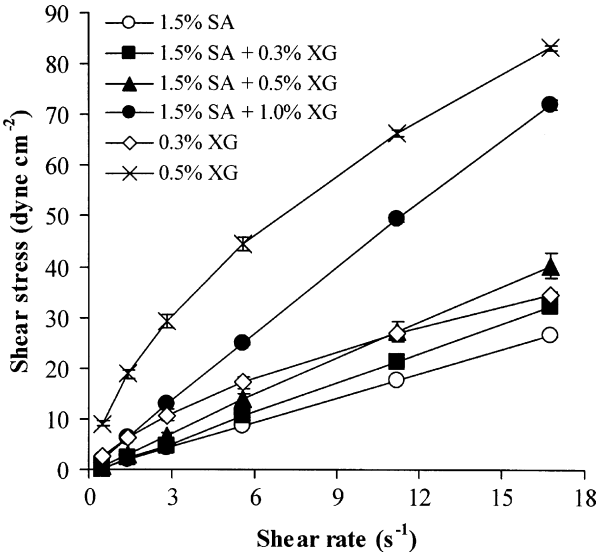

Fig. 1. Rheograms of SA and XG–SA dispersions. Each value is the mean ± S.D., $n = 3$.

that the flow behavior of these dispersions was Newtonian flow. On the other hand, more than unity of N values was found in XG dispersions that represented pseudoplastic flow. This suggested that incorporation of XG did not affect the flow behavior of SA dispersion. Viscosity coefficient of SA dispersion increased significantly ($P < 0.05$) with increasing amount of XG. However, the viscosity coefficient of the composite dispersion was less than that of XG dispersion. This indicated that SA and XG had a viscosity synergism, but the self-association gel structure of XG was broken down when incorporating with SA. Generally XG had a trisaccharide side chain that was able to form intermolecular association. This resulted in the formation of a complex network of weakly bound molecules, which was called as a rigid rod (Sworn, 2000). Incorporating XG into SA dispersion cause a loss of a complex network of XG, which led to a decrease of viscosity of XG, but XG could still form small aggregates that can be visually observed. However, small aggregates of XG and SA molecules could form intermolecular bonding, such as hydrogen bonding, by an interaction of hydroxyl and carboxyl groups of such polymers, resulting in an increasing of viscosity of the composite dispersion. From these results, the possible synergistic type of XG and SA was phase-separated networks combined with coupled networks (Gruber and Konish, 1999).

Table 1
Rheological properties of SA and XG–SA composite dispersions

Component	N	Viscosity coefficient [(dyne cm^{-2})^N s]	Type of flow
1.5% (w/v) SA	0.96 ± 0.03	1.42 ± 0.11	Newtonian
+0.3% (w/v) XG	0.93 ± 0.02	1.54 ± 0.10	Newtonian
+0.5% (w/v) XG	0.97 ± 0.02	2.25 ± 0.23	Newtonian
+1% (w/v) XG	1.01 ± 0.03	4.57 ± 0.51	Newtonian
0.3% (w/v) XG	1.38 ± 0.02	8.88 ± 1.07	Pseudoplastic
0.5% (w/v) XG	1.60 ± 0.02	75.91 ± 9.15	Pseudoplastic

Data are mean ± S.D., $n = 3$.

Molecular interaction between XG and SA in dispersion could be predicted using structure of both polymers. The structure of XG consists of the primary chain of β-D-(1,4)-glucose and a trisaccharide side chain (Fig. 2a), while SA composes of β-D-mannuronic acid residues (Fig. 2b) that are the main composition of SA used in this study (US Pharmacopeia XXII, 1990). Similar to the interaction between XG and other polysaccharides, such as galactomannan (Chandrasekaran and Radha, 1997), hydroxyl groups on the primary chain (point A) and the side chain (point B) of XG (Fig. 2c) could form intermolecular hydrogen bonding with carboxyl groups of SA. Moreover, the formation of hydrogen bonding could possibly occur between the carboxyl groups on the terminal side chain of XG and hydroxyl groups of SA (point C). It was suggested that the predicted molecular interaction led to viscosity synergism of SA with XG.

3.2. FTIR studies

Molecular interaction of SA and XG in calcium alginate beads was investigated using FTIR spectroscopy. FTIR spectra of SA showed the peaks around 3435, 1615, 1418, and 1031 cm^{-1}, indicating the stretching of O–H, COO$^-$ (asymmetric), COO$^-$ (symmetric), and C–O–C, respectively (Fig. 3a). The cross-linking process with calcium ion caused an obvious shift to higher wavenumber and a decrease in intensity of COO$^-$ stretching peaks, and a decrease in intensity of 1031 cm^{-1} peak of SA (Fig. 3b). This indicated that an ionic bonding between calcium ion and carboxyl groups of SA and a partial covalent bonding between calcium and oxygen atom of ether groups, respectively. This result is in agreement with the previous studies (Sartori et al., 1997; Puttipipatkhachorn et al., 2005). Incorporation of XG into the calcium alginate beads obviously provided a shift to lower wavenumber and the lower intensity of COO$^-$ stretching peak at 1635 cm^{-1}. The peak at 1433 cm^{-1} disappeared and C–O–C strenching peak at 1031 cm^{-1} shifted to 1024 cm^{-1} (Fig. 3c–e). Moreover, the O–H stretching peak at 3435 cm^{-1} of the beads had a greater intensity and a narrower peak when adding XG. The above phenomenon suggested that SA and XG could form intermolecular hydrogen bonding (Nakanishi and Solomon, 1977; Wanchoo and Sharma, 2003). The formation of hydrogen bonding that possibly occurred in dispersion before cross-linking took place demonstrated a possibility of molecular interaction between XG and SA as predicted in Section 3.1. Moreover, it can also be seen that FTIR spectra of calcium alginate beads with XG did not show the peaks of XG, although 1%XG was used. It is possible to explain that XG may form an ionic bonding with calcium ions as well.

FTIR spectra of DCA beads and XG–DCA beads were also investigated as shown in Fig. 4. The spectra of the DCA beads showed the peaks around 1575–1386 cm^{-1} of DS, and a remarkable shift to lower wavenumber of COO$^-$ (asymmetric) and C–O–C stretching peaks of calcium alginate (Fig. 4b). This result was similar to our previous studies (Pongjanyakul et al., 2006). It can be described that amino groups of diclofenac could protonate in SA dispersion and then interacted with carboxyl and ether groups of alginate before cross-linking process. Incorporation of XG at all levels into the DCA beads did not affect the

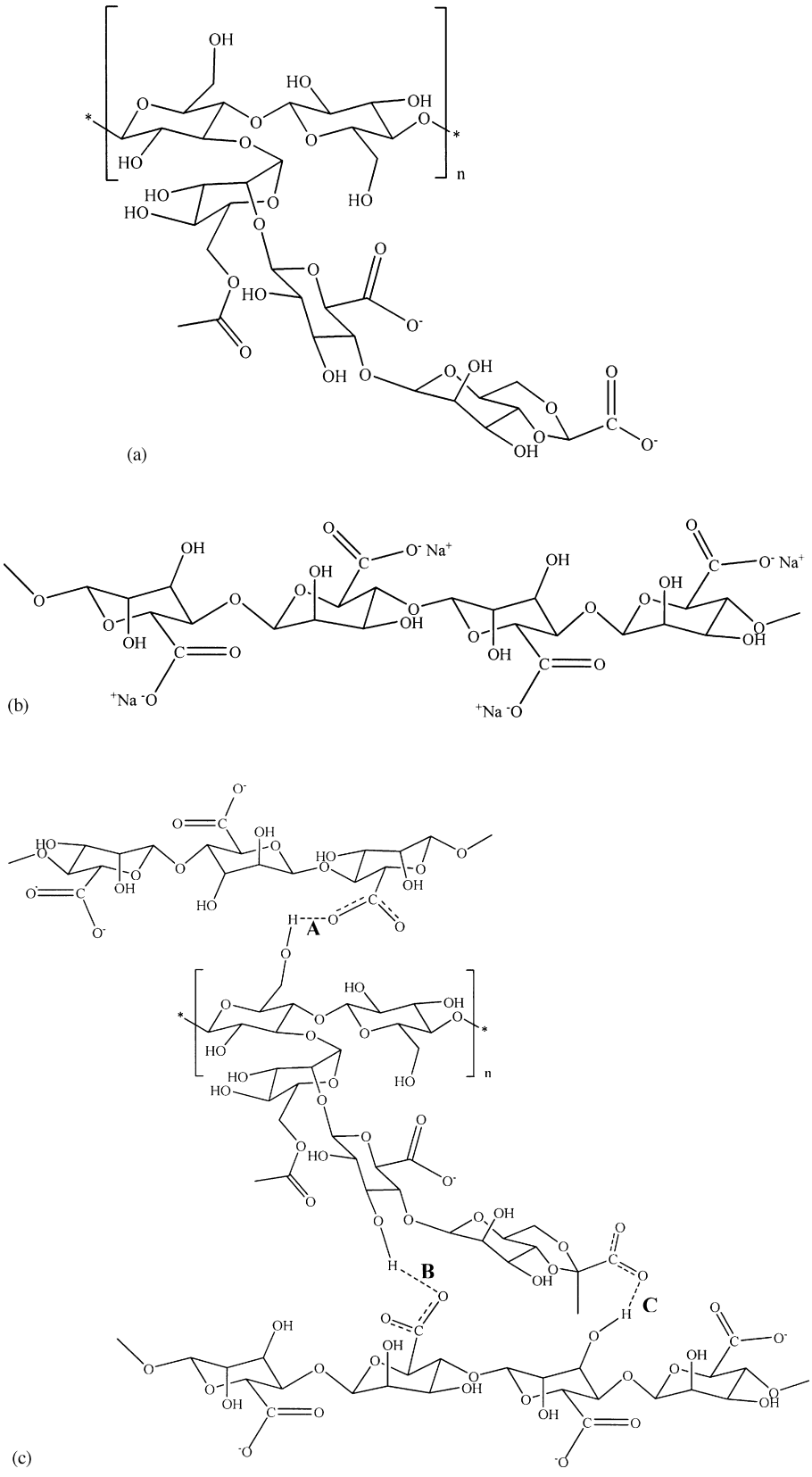

Fig. 2. Molecular structures of XG (a) and SA (b), and possible molecular interaction between XG and SA by the formation of intermolecular hydrogen bonding at points A, B, or C (c).

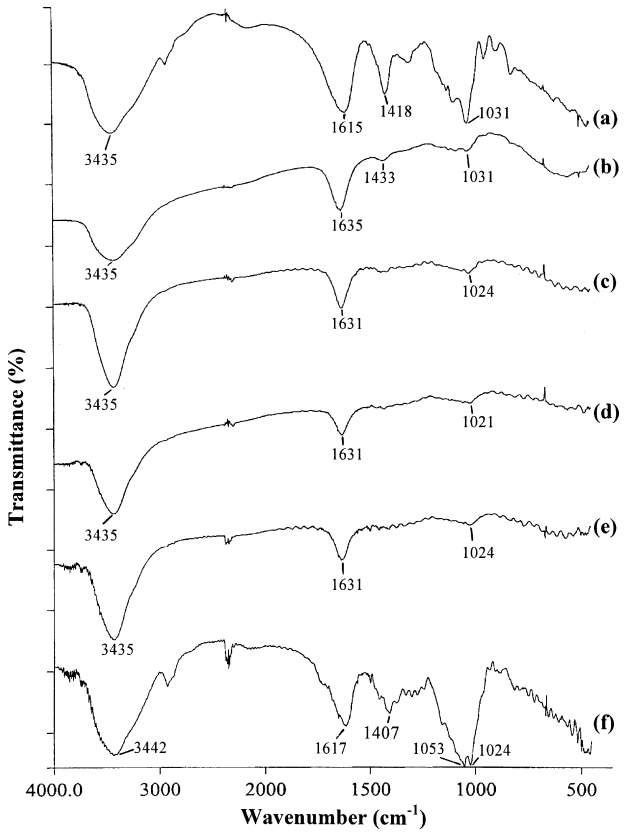

Fig. 3. FTIR spectra of SA (a), calcium alginate beads prepared using 0.0% (b), 0.3% (c), 0.5% (d) and 1.0% (w/v) XG (e), and XG (f).

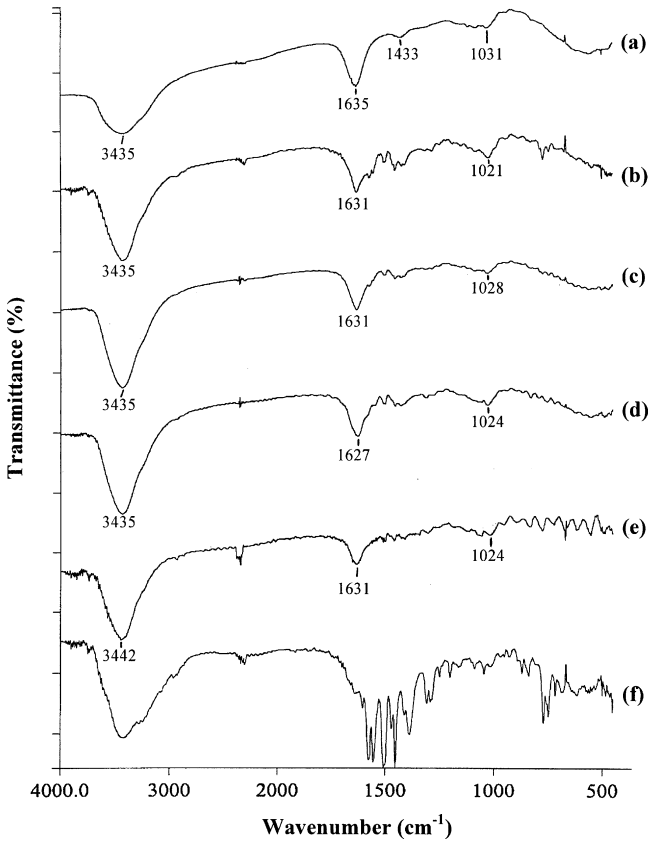

Fig. 4. FTIR spectra of calcium alginate beads (a), DCA beads prepared using 0.0% (b), 0.3% (c), 0.5% (d) and 1.0% (w/v) XG (e), and DS (f).

peaks of the DCA beads (Fig. 4c–e). Moreover, these spectra were similar to the spectra of calcium alginate beads with XG in Fig. 3c–e. This suggested that the gel matrix structure of XG and calcium alginate in the beads was still formed after incorporating DS. These findings indicated that molecular interaction between SA and XG was able to create a complex matrix structure in the calcium alginate beads with or without DS, which caused a change in characteristics of the DCA beads.

3.3. DSC studies

The DSC thermogram of DS showed an endothermic peak at 55 °C (Fig. 5a). This was due to the evaporation of the water of crystallization (Palomo et al., 1999). The sharp exothermic peak of DS at 280 °C and a small endothermic peak at 284 °C indicated an oxidation reaction between DS and oxygen in air environment and a melting of the compound, respectively (Tudja et al., 2001). SA and XG showed decomposition peak around 250 and 280 °C, respectively (Fig. 5b and c). The calcium alginate beads presented a broad endothermic peak at 70 °C and the exothermic peak of SA was absent (Fig. 5d), indicating the interaction of SA and calcium ion (Fernández-Hervás et al., 1998; Puttipipatkhachorn et al., 2005). This was similar to a DSC thermogram of the DCA beads (Fig. 5f). This suggested that DS in amorphous form was dispersed in the calcium alginate matrix (Benoit et al., 1986). Incorporating XG into the calcium alginate beads and the DCA beads (Fig. 5e and g) presented no different thermogram. This indicated that incorporation of XG did not affect the thermal property of the DCA beads.

3.4. Physical properties of the composite DCA beads

The physical characteristics of the XG–DCA beads are shown in Table 2. The mean diameters of the XG–DCA beads tended to increase with increasing content of XG added. The DCA beads prepared were spherical as shown in SEM photographs (Fig. 6a and c). The DS entrapment efficiency of the XG–DCA beads increased significantly ($P < 0.05$) with increasing amount of XG. It was indicated that the interaction of XG with SA caused an increase in barrier for preventing a water leakage from the beads during the preparation period (Dashevsky, 1998). These led to reduce the drug loss from the beads. To compare with the effect of sodium starch glycolate (SSG) on DS entrapment efficiency of the DCA beads, which was reported previously (Puttipipatkhachorn et al., 2005), the XG–DCA beads provided higher DS entrapment efficiency than the SSG–DCA beads. This was the effect of polymer structure and molecular weight. SSG is a linear polymer with molecular weight around $(5–10) \times 10^5$, whereas XG had a trisaccharide side chain polymer with high molecular weight (2×10^6). Additionally, cations tend to salt out the hydrophobic site of XG helix to form the junction zones that could produce a slight increase in viscosity (Gruber, 1999), and the XG might be cross-linked in the high concentration of Ca^{2+}. From these reasons, XG could form denser

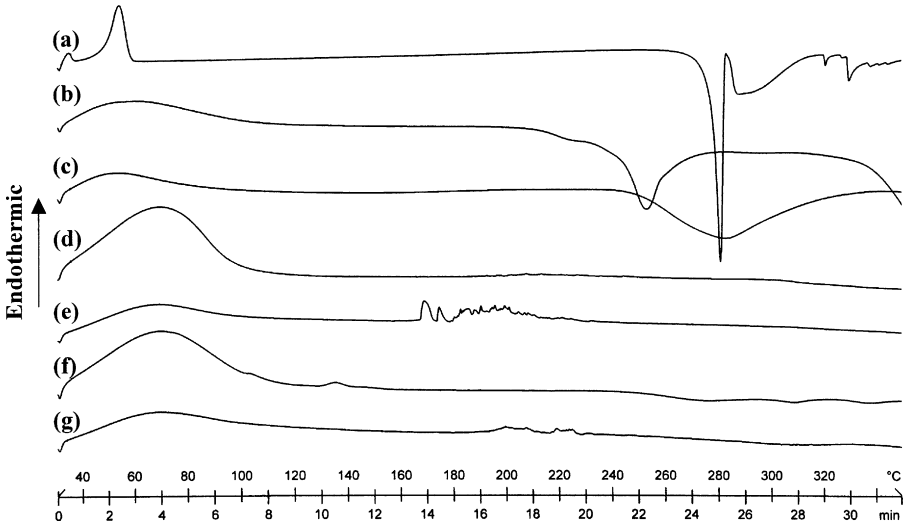

Fig. 5. DSC thermograms of DS (a), SA (b), XG (c), calcium alginate beads (d), calcium alginate beads prepared using 1.0% (w/v) XG (e), DCA beads (f), and DCA beads prepared using 1.0% (w/v) XG (g).

matrix of the beads than SSG, leading to higher entrapment of DS.

3.5. Water uptake and swelling of the composite DCA beads

The water uptake of the XG–DCA beads in pH 6.8 phosphate buffer is shown in Fig. 7a. The %water uptake of the DCA beads in pH 6.8 phosphate buffer increased with increasing time of testing. The XG–DCA beads provided obviously higher %water uptake than the DCA beads. The water uptake of the DCA beads increased as the added amount of XG increased. However, the water uptake tended to decrease when the amount of added XG increased to 1%. The %water uptake in distilled water was significantly lower ($P < 0.05$) than that in pH 6.8 phosphate buffer (Fig. 7b). The equilibrium time of water uptake in distilled water of the DCA beads was around 30–60 min. The water uptake of the DCA beads and 0.3%XG–DCA beads was comparable, but that of 0.5% and 1%XG–DCA beads was statistically higher ($P < 0.05$) when compared with the DCA beads.

The swelling profiles of the XG–DCA beads in pH 6.8 phosphate buffer and distilled water are shown in Fig. 8. In pH 6.8 phosphate buffer, the swelling equilibrium time of the DCA beads was approximately 120 min (Fig. 8a). The %swelling of the DCA beads increased with addition of XG. The swelling rate of the DCA beads in pH 6.8 phosphate buffer could be obtained from the slope of the relationship between the %swelling and the square root of time (Lee and Peppas, 1987; Puttipipatkhachorn et al., 2005). This relationship provided a good linearity with R^2 more than 0.96 when analyzed by linear regression analysis (Table 2). The swelling rate of the XG–DCA beads tended to increase when compared with the DCA beads, but 0.5%XG–DCA beads showed a comparable swelling rate with 1.0%XG–DCA beads. Using distilled water, the swelling rate of the DCA beads cannot be estimated because of the lower swelling of the DCA beads in this medium. However, the %swelling of the DCA beads remarkably increased with increasing amount of XG (Fig. 8b).

The water uptake and swelling of the DCA beads in pH 6.8 phosphate buffer was higher than those in distilled water because calcium ions cross-linked with alginate were rapidly exchanged with sodium ions in phosphate buffer (Østberg et al., 1994). The partial formation of SA induced water uptake into the beads. Moreover, calcium alginate gels could be solubilized by the addition of phosphate ion, which acted as calcium ions complexing agent at a pH above 5.5 (Remuñán-López and Bodmeier, 1997). Incorporation of XG into the DCA beads pro-

Table 2
Characteristics of the composite DCA beads

Components	Mean diameter[a] (mm)	EE[b] (%)	pH 6.8 phosphate buffer			Distilled water	
			Swelling rate[c] (% min^{-1})	Release rate[b] (% min^{-1})	Lag time[b] (min)	Release rate[b] (% min$^{-1/2}$)	Matrix erosion[b] (%)
1.5% (w/v) SA	1.37 ± 0.11	39.8 ± 2.7	21.7 ± 3.6 (R^2 = 0.98)	1.28 ± 0.05 (R^2 = 0.98)	19.4 ± 0.7	3.12 ± 0.09 (R^2 = 0.99)	59.1 ± 0.1
+0.3% (w/v) XG	1.53 ± 0.12	42.1 ± 3.0	18.6 ± 4.2 (R^2 = 0.98)	1.57 ± 0.03 (R^2 = 0.98)	25.6 ± 1.4	2.31 ± 0.03 (R^2 = 0.99)	60.4 ± 0.2
+0.5% (w/v) XG	1.37 ± 0.12	47.0 ± 1.6	25.6 ± 1.2 (R^2 = 0.96)	1.78 ± 0.12 (R^2 = 0.99)	26.7 ± 1.0	3.75 ± 0.04 (R^2 = 0.99)	46.6 ± 0.3
+1% (w/v) XG	1.50 ± 0.11	50.9 ± 1.5	23.5 ± 2.5 (R^2 = 0.99)	1.33 ± 0.08 (R^2 = 0.98)	30.2 ± 1.3	3.91 ± 0.02 (R^2 = 0.99)	42.8 ± 0.1

EE: entrapment efficiency of DS. R^2: determination coefficient.
[a] Data are mean ± S.D., n = 250.
[b] Data are mean ± S.D., n = 3.
[c] Data are mean ± S.D., n = 5.

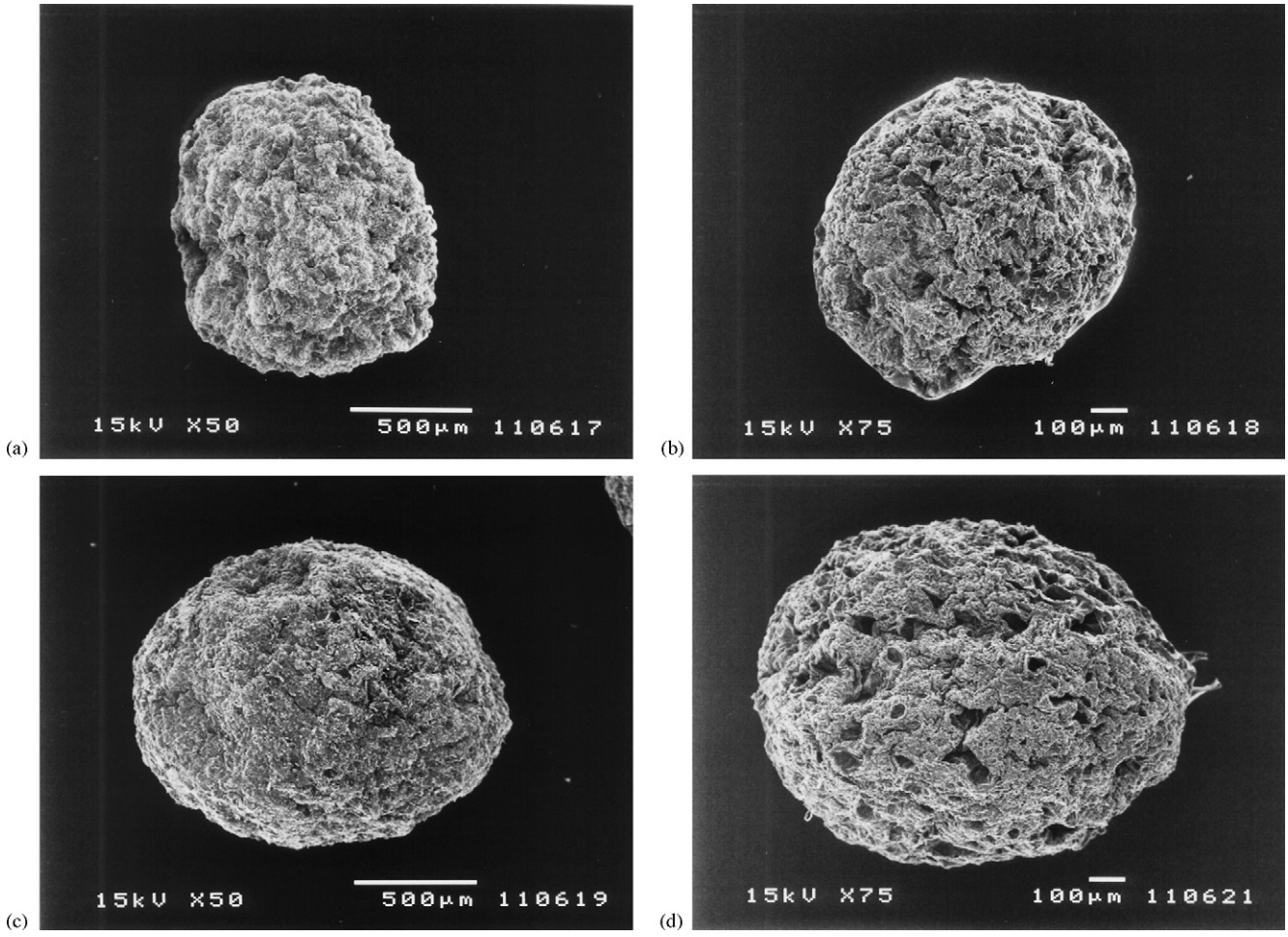

Fig. 6. SEM photographs of DCA beads, and 1.0%XG–DCA beads before (a and c) and after (b and d) release studies in distilled water.

moted the water uptake and swelling properties in pH 6.8 phosphate buffer because XG provided higher water uptake capacity than SA (Bertram and Bodmeier, 2006). However, 1%XG–DCA beads gave lower water uptake and comparable swelling rate when compared with 0.5%XG–DCA beads. It was possible to explain that higher amount of XG in swollen 1%XG–DCA beads increased internal viscosity and gave more rigid matrix gel structure due to interaction of XG and SA. This also included the interaction of XG with Ca^{2+}. In distilled water, the effect of XG on water uptake and swelling was clearly demonstrated because the DCA beads existed as a stable polymer matrix. The increase in water uptake and swelling of the DCA beads increased with increasing amount of added XG. This can be attributed to the chemical structure of XG molecules having negative charge of carboxyl groups on trisaccharide side chains, which caused an increase of repulsive forces and expansion of the matrix. This resulted in greater water absorption capacity (Elçin, 1995).

The effect of XG, branched polymer, and SSG, linear polymer, on water uptake and swelling of the DCA beads was also compared using the results of our previous study (Puttipipatkhachorn et al., 2005). The XG–DCA beads gave higher water uptake and swelling in both media than the SSG–DCA beads. This indicated that incorporating of the different polymer into the DCA beads affected water uptake and swelling, although such polymers could form intermolecular hydrogen bonding with SA. However, high molecular weight of XG and small aggregates of XG dispersed in the DCA matrix gave greater water sorption capacity of the XG–DCA beads, leading to increasing of swelling.

3.6. *In vitro release of the composite DCA beads*

The release profiles of DS from the XG–DCA beads in pH 6.8 phosphate buffer and distilled water are shown in Fig. 9. The release profile of DS in pH 6.8 phosphate buffer showed a sigmoidal profile with a complete release (Fig. 9a) and the disintegration of the swollen beads occurred around 75–90 min of the test. A lag time and a release rate of DS were obtained from fitting the data into zero order model, which a good linearity with R^2 higher than 0.98 was found. This indicated swelling controlled mechanism. The higher the added XG content, the longer the lag time was obtained (Table 2). The release rate of the 0.3% and 0.5%XG–DCA beads was significantly higher ($P < 0.05$) than that of the DCA beads and the decrease of DS release rate was observed in 1%XG–DCA beads. In distilled water, incomplete release of DS for 8 h was obtained (Fig. 9b). The release of DS in this medium did not show the lag time and can be described using Higuchi's model. The 0.3%XG–DCA beads gave lower release

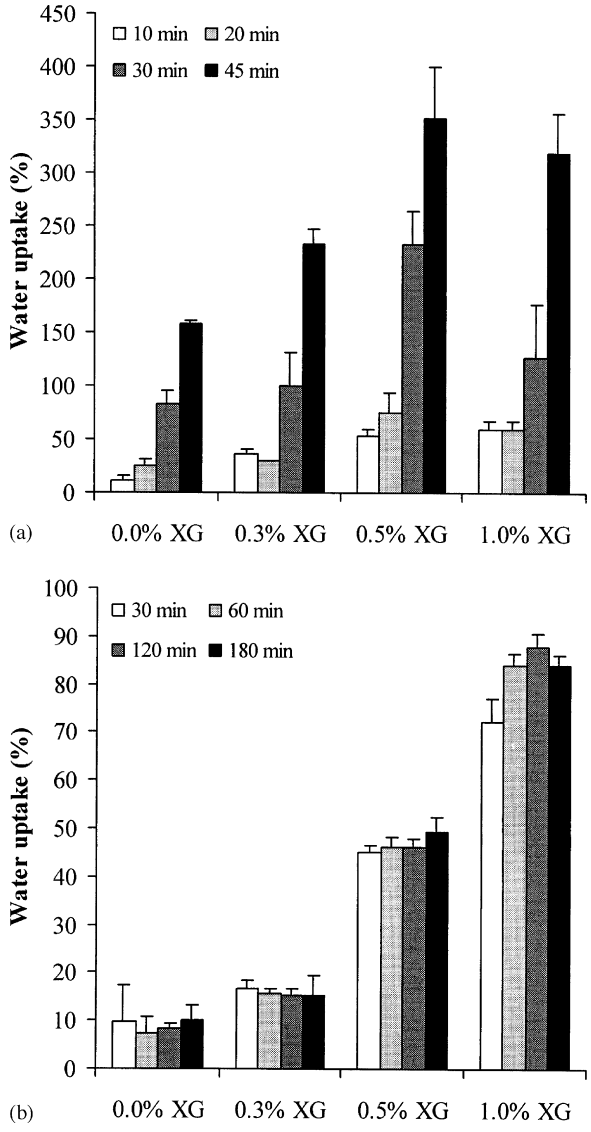

Fig. 7. Water uptake of DCA beads prepared using different contents of XG in pH 6.8 phosphate buffer (a) and distilled water (b). Each value is the mean ± S.D., $n = 3$.

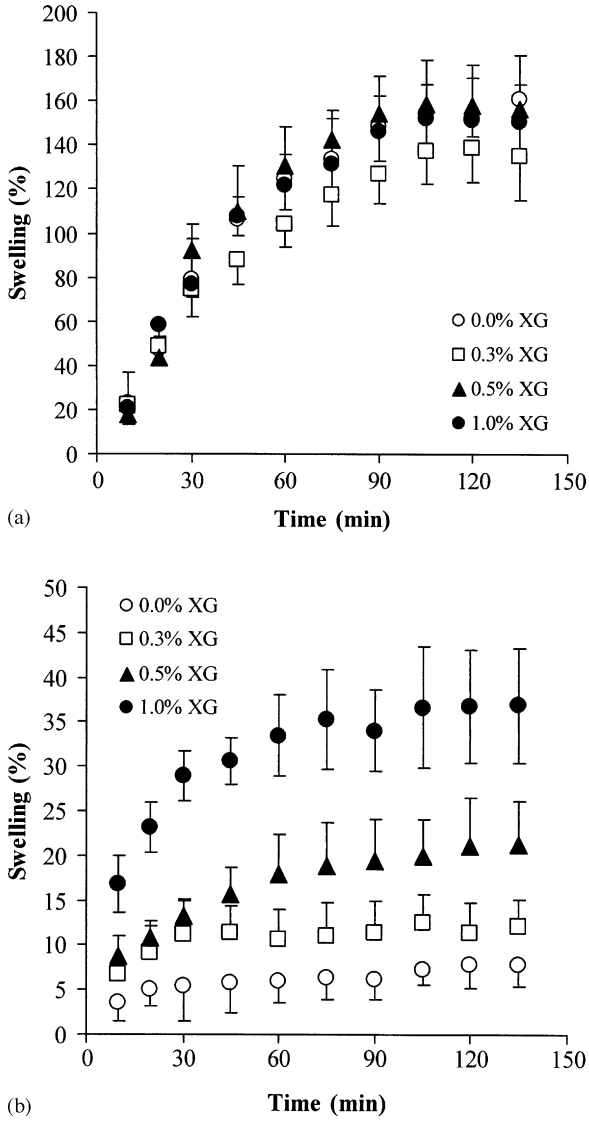

Fig. 8. Swelling profiles of DCA beads prepared using different contents of XG in pH 6.8 phosphate buffer (a) and distilled water (b). Each value is the mean ± S.D., $n = 5$.

rate than the DCA beads, whereas the release rate of 0.5% and 1.0%XG–DCA beads was statistically higher ($P < 0.05$) than that of the DCA beads (Table 2). The matrix erosion of the DCA beads was significantly decreased ($P < 0.05$) when using 0.5 and 1%XG (Table 2). SEM photographs showed the erosion of the surface of the DCA beads after release testing in distilled water (Fig. 6b), whereas many larger pores on the surface of the 1%XG–DCA beads were found (Fig. 6d). The erosion of the DCA beads could be observed because a residual alginate could release from the beads (Murata et al., 1993), which occurred from a small amount of calcium ion released in distilled water (Østberg et al., 1994). Moreover, XG could erode in the form of small aggregate, resulting in large pore formations on the DCA beads.

The release of DS from the DCA beads in pH 6.8 phosphate buffer was depressed by the formation of the gel layer at the initial stage but gradually enhanced by the increasing water content and the erosion of the swollen gel phase at the later stage (Sugawara et al., 1994). This can be described by using the ion exchange between calcium ion in the beads and sodium ion in the medium. Calcium ions interacted with carboxylic groups in alginate, but not participating in the egg-box formation, are preferentially released through ion exchange with sodium ion in the medium. Almost negligible alginate disintegration at this stage was probably due to the relatively stable association of calcium ions with polyguluronate sequences, which served as stable cross-linking points within the gels. Alginate disintegration occurred when the calcium ion in the egg-box structure started to release for exchange with sodium ion (Kikuchi et al., 1997). Furthermore, the lag time of release profile occurred because the solubility of DS was decreased with the presence of sodium ions. This can be attributed to the common ion effect (Sheu et al., 1992). Incorporation of XG caused higher water uptake and swelling, but gave longer lag time of DS release.

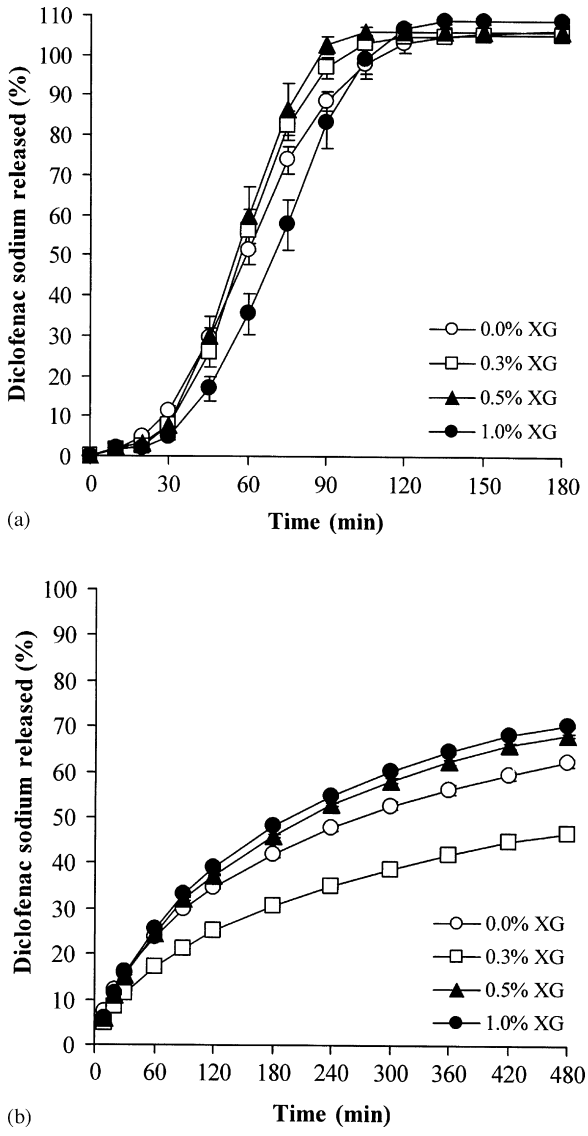

Fig. 9. DS release profiles of DCA beads prepared using different contents of XG in pH 6.8 phosphate buffer (a) and distilled water (b). Each value is the mean ± S.D., $n = 3$.

This was due to the entrapment of DS molecules in high tortuosity swollen beads, which resulted from the complex formation of SA and XG. Moreover, the longer diffusion pathlength may be occurred due to the high swelling of the DCA beads. However, high concentration of DS in the swollen beads brought about a pulse release of DS, which led to a faster DS release in the 0.3% and 0.5%XG–DCA beads. A slower release rate of the 1%XG–DCA beads was found because higher content of XG tended to decrease water uptake and produced higher tortuosity of the swollen beads.

The release of DS from the DCA beads in distilled water was slower than that in pH 6.8 phosphate buffer because the DCA beads was stable with the small amount of calcium released (Østberg et al., 1994). Thus, the release mechanism of DS from the beads was matrix diffusion-controlled. The 0.3%XG–DCA beads provided a similar water uptake and swelling with the DCA beads, but could retard the release of DS, suggesting that greater tortuosity in the bead matrix could be formed due to interaction of XG and SA. However, a faster release rate of 0.5% and 1%XG–DCA beads was found. This was due to higher water uptake and erosion of small aggregates from the surface of the beads. In addition, incorporating XG into the DCA beads caused a decrease of matrix erosion. This also indicated interaction of XG and SA in the DCA beads and the erosion of XG from the DCA beads occurred mainly on the surface of the DCA beads.

The drug release behavior and the water uptake of the XG–DCA composite beads in distilled water showed different results when compared to those of the SSG–DCA beads, which were previously reported (Puttipipatkhachorn et al., 2005). SSG could accelerate DS release from the DCA beads although the SSG–DCA beads gave lower water uptake than the XG–DCA beads. This suggested than SSG could create water-filled channels throughout the bead matrix, which many small pores on the surface of the beads could be observed. On the other hand, small aggregate of XG in the XG–DCA beads give higher water uptake capacity, but created greater tortuosity of water-filled channels. The matrix erosion was occurred mainly on the surface of the XG-DCA beads. These led to slower release of the XG–DCA beads.

4. Conclusions

Incorporation of XG into the DCA beads caused a change in matrix structure of the beads due to intermolecular hydrogen bonding between XG and SA, and formation of small aggregates of XG after dispersing into SA dispersion. The XG–DCA beads gave higher entrapment efficiency of DS and increased water uptake and swelling in pH 6.8 phosphate buffer and distilled water. A longer lag time and a higher release rate of DS in pH 6.8 phosphate buffer were found. In contrast, the 0.3%XG–DCA beads could retard the drug release in distilled water. However, higher content of XG in the DCA beads increased the release rate of DS. This was due to erosion of small aggregates of XG on the surface of the DCA beads. This finding suggested that XG could modulate physicochemical properties and drug release of the DCA beads, which based on the existence of molecular interaction of XG and SA.

Acknowledgements

The authors wish to thank P. Sri-udon and S. Kanjanabat for laboratory assistance and Faculty of Pharmaceutical Sciences, Khon Kaen University, Khon Kaen, Thailand for technical supports.

References

Almeida, P.F., Almeida, A.J., 2004. Cross-linked alginate-gelatin beads: a new matrix for controlled release of pindolol. J. Control. Release 97, 431–439.

Benoit, J.P., Courteille, F., Thies, C., 1986. A physicochemical study of the morphology of progesterone loaded poly(D,L-lactide) microspheres. Int. J. Pharm. 29, 95–102.

Bertram, U., Bodmeier, R., 2006. In situ gelling, bioadhesive nasal inserts for extended drug delivery: in vitro charaterization of a new nasal dosage form. Eur. J. Pharm. Sci. 27, 62–71.

Chandrasekaran, R., Radha, A., 1997. Molecular modeling of xanthan: galactomannan interactions. Carbohydr. Polym. 32, 201–208.

Costa, P., Lobo, J.M.S., 2001. Modeling and comparison of dissolution profiles. Eur. J. Pharm. Sci. 13, 123–133.

Dashevsky, A., 1998. Protein loss by the microencapsulation of an enzyme (lactase) in alginate beads. Int. J. Pharm. 161, 1–5.

Draget, K.I., 2000. Alginates. In: Philips, G.O., Williams, P.A. (Eds.), Handbook of Hydrocolloids. Woodhead Publishing, Cambridge, pp. 379–395.

Elçin, Y.M., 1995. Encapsulation of urease enzyme in xanthan–alginate spheres. Biomaterials 16, 1157–1161.

Fernández-Hervás, M.J., Holgado, M.A., Fini, A., Fell, J.T., 1998. In vitro evaluation of alginate beads of a diclofenac salt. Int. J. Pharm. 163, 23–34.

Grant, G.T., Morris, E.R., Rees, D.A., Smith, P.J.C., Thom, D., 1973. Biological interaction between polysaccharides and divalent cations: the egg-box model. FEBS Lett. 32, 195–198.

Gruber, J.V., 1999. Polysaccharide-based polymers in cosmetics. In: Goddard, E.D., Gruber, J.V. (Eds.), Principles of Polymer Science and Technology in Cosmetics and Personal Care. Marcel Dekker, New York, pp. 325–389.

Gruber, J.V., Konish, P.N., 1999. Building aqueous viscosity through synergistic polymer–polymer interactions. In: El-Nokaly, M.A., Soini, H.A. (Eds.), Polysaccharide Application: Cosmetics and Pharmaceuticals. American Chemical Society, Washington, pp. 252–261.

Hwang, S.J., Rhee, G.J., Lee, K.M., Oh, K.H., Kim, C.K., 1995. Release characteristics of ibuprofen from excipient-loaded alginate gel beads. Int. J. Pharm. 116, 125–128.

Kikuchi, A., Kawabuchi, M., Sugihara, M., Sakurai, Y., Okano, T., 1997. Pulsed dextran release from calcium-alginate gel beads. J. Control. Release 47, 21–29.

Kim, M.S., Park, G.D., Jun, S.W., Lee, S., Park, J.S., Hwang, S.J., 2005. Controlled release tamsulosin hydrochloride from alginate beads with waxy materials. J. Pharm. Pharmacol. 57, 1521–1528.

Lee, P.I., Peppas, N.A., 1987. Prediction of polymer dissolution in swellable controlled-release systems. J. Control. Release 6, 207–215.

Martin, A., 1993. Physical Pharmacy, 4th ed. Lea & Febiger, Philadelphia, pp. 453–476.

Murata, Y., Miyamoto, E., Kawashima, S., 1996. Additive effect of chondroitin sulfate and chitosan on drug release from calcium-induced alginate gel beads. J. Control. Release 38, 108–110.

Murata, Y., Nakada, K., Miyamoto, E., Kawashima, S., Seo, S.H., 1993. Influence of erosion of calcium-induced alginate gel matrix on the release of Brilliant Blue. J. Control. Release 23, 21–26.

Murata, Y., Tsumoto, K., Kofuji, K., Kawashima, S., 2002. Effect of natural polysaccharide addition on drug release from calcium-induced alginate gel beads. Chem. Pharm. Bull. 51, 218–220.

Nakanishi, K., Solomon, P.H., 1977. Infrared Absorption Spectroscopy, 2nd ed. Holden-Day Inc., San Francisco.

Østberg, T., Lund, E.M., Graffner, C., 1994. Calcium alginate matrices for oral multiple unit administration. IV. Release characteristics in different media. Int. J. Pharm. 112, 241–248.

Palomo, M.E., Ballesteros, M.P., Frutos, P., 1999. Analysis of diclofenac sodium and derivatives. J. Pharm. Biomed. Anal. 21, 83–94.

Pongjanyakul, T., Sungtongjeen, S., Puttipipatkhachorn, S., 2006. Modulation of drug release from glyceryl palmitostearate-alginate beads via heat treatment. Int. J. Pharm. 319, 20–28.

Puttipipatkhachorn, S., Pongjanyakul, T., Priprem, A., 2005. Molecular interaction in alginate beads reinforced with sodium starch glycolate or magnesium aluminum silicate, and their physical characteristics. Int. J. Pharm. 293, 51–62.

Remuñán-López, C., Bodmeier, R., 1997. Mechanical, water uptake and permeability properties of crosslinked chitosan glutamate and alginate films. J. Control. Release 44, 215–225.

Santos, H., Veiga, F., Pina, M.E., Sousa, J.J., 2005. Compaction, compression and drug release properties of diclfenac sodium and ibuprofen pellets comprising xanthan gum as a sustained release agent. Int. J. Pharm. 295, 15–27.

Sartori, C., Finch, D.S., Ralph, B., 1997. Determination of the cation content of alginate thin films by FTIR spectroscopy. Polymer 38, 43–51.

Sheu, M.T., Chou, H.L., Kao, C.C., Liu, C.H., Sokoloski, T.D., 1992. Dissolution of diclofenac sodium from matrix tablets. Int. J. Pharm. 85, 57–63.

Sugawara, S., Imai, T., Otagiri, M., 1994. The controlled release of prednisolone using alginate gel. Pharm. Res. 11, 272–277.

Sujja-areevath, J., Munday, D.L., Cox, P.J., Khan, K.A., 1996. Release characteristics of diclfenac sodium from encapsulated natural gum mini-matrix formulations. Int. J. Pharm. 139, 53–62.

Sworn, G., 2000. Xanthan gum. In: Philips, G.O., Williams, P.A. (Eds.), Handbook of Hydrocolloids. Woodhead Publishing, Cambridge, pp. 103–115.

Talukdar, M.M., Kinget, R., 1995. Swelling and drug release behaviour of xanthan gum tablets. Int. J. Pharm. 120, 63–72.

Tudja, P., Khan, M.Z.I., Meštrović, E., Horvat, M., Golja, P., 2001. Thermal behaviour of diclofenac sodium: decomposition and melting characteristics. Chem. Pharm. Bull. 49, 1245–1250.

US Pharmacopeia XXII, 1990. United States Pharmacopeia Convention Inc., Rockville, MD, 1978 pp.

Wade, A., Weller, P.J., 1994. Handbook of Pharmaceutical Excipients, 2nd ed. The American Pharmaceutical Association, Washington and The Pharmaceutical Press, London, pp. 562–563.

Wanchoo, R.K., Sharma, P.K., 2003. Viscometric study on the compatibility of some water-soluble polymer–polymer mixtures. Eur. Polym. J. 39, 1481–1490.

Wang, K., He, Z., 2002. Alginate-konjac glucomannan-chitosan beads as controlled release matrix. Int. J. Pharm. 244, 117–126.

Zeng, W.M., 2004. Oral controlled release formulation for highly water-soluble drugs: drug–sodium alginate–xanthan gum–zinc acetate matrix. Drug Dev. Ind. Pharm. 30, 491–495.